THERMAL ANALYSIS OF HEAT PIPE SHELL-FIN STRUCTURES WITH SELECTIVE COATINGS UNDER RADIATION

Joon Hong Boo

(Received August 18, 1992)

The purpose of this study is to investigate the thermal response of a heat pipe shell-fin structure that is selectively coated and is subject to uneven radiation from upper and lower sides. Such a structure would arise when fins are attached to opposing sides of the condenser or evaporator section of heat pipes to enhance the heat transfer performance. Typical examples include radiators for space applications and solar energy collectors for water heating. The temperature distribution in the circumferential direction of the heat pipe shell as well as that in the fin is examined via theoretical modeling and numerical analysis. The model accounts for the effects of selective coatings. Both steady-state and transient solution procedures are presented. Examination of the steady-state results justifies the use of a thermally-lumped formulation for the heat pipe shell region. The effect of fin width is investigated as a typical design variable. The fin efficiency and the collector efficiency are also presented as functions of heat pipe operating temperature and fin widith. The influence of the surface properties on the thermal performance of the heat pipe shell-fin structure are also examined.

Key Words: Heat Pipe, Fin Radiator, Collector, Selective Coating, Steady State, Fransient, Thermal Performance

NOMENCLATURE

A : Area, (m^2)
b : Thickness of a fin, (m)
Bi : Biot number, dimensionless
c : Specific heat at constant volume, (J/kg·K)
$E_{b,r}$: Blackbody emissive power, (W/m^2)
Fo : Fourier number
G_r : Irradiation from the sun and space, (W/m^2)
G_{sun} : Irradiation from the sun, (W/m^2)
G_{space} : Irradiation from the space, (W/m^2)
h : Convective heat transfer coefficient, (W/m·K)
k : Thermal conductivity, (W/m·K)
q : Heat flow ; amount of heat transfer, (W)
Q : Heat transfer rate, (W)
r : Radius, (m)
T : Temperature, (K)
V : Volume, (m^3)
W : Width of the fin, (m)
x : Length in the fin direction, (m)

Greek Symbols
α : Thermal diffusivity, (m^2/K)
α_r : Absorptivity, dimensionless
δ : Thickness of heat pipe shell, (m)
Δ : Change,
ϵ : Emissivity, dimensionless
ζ : Thickness-to-radius ratio of heat pipe shell
η : Efficiency
θ : Dimensionless temperature
ξ : Dimensionless distance, x/W
ξ_r : Dimensionless arc length, $r_o\Delta\phi/W$
ρ : Density, (kg/m^3)
σ : Stefan-Boltzmann constant, ($5.67\times10^{-8}W/m^2\cdot K^4$)
ϕ : Angle

Superscripts
(n) : (n)th time step
(r) : (r)th iteration

Subscripts
o,ref : Reference state
v : Refers to vapor
w : Refers to the liquid-vapor interface
ϕ : Angular direction
∞ : Ambient surroundings

*Department of Aeronautical and Mechanical Engineering Hankuk Aviation University 200-1 Hwajun, Koyang, Kyungki-do, Seoul 411-791, Korea

1. INTRODUCTION

In many engineering applications associated with heat pipes, a full analysis is complex in nature because three different phases are present—solid, liquid, and vapor—and three different heat transfer modes occur—conduction, convection, and radiation. The number of relevant dimensions is an additional factor that increases the complexity of the mathematical model. A simplified mathematical model is thus desired that can help reduce the complexity of the problem of investigating the thermal response of heat pipe structures.

The geometry and dimensions of the model in this study are from the base design of a high-capacity heat pipe radiator panel presented by Colwell and Hartley(1988) and are described in Fig. 1. Since the model structure is exposed to uneven radiation from upper and lower sides, the temperature variation in the circumferential direction of the heat pipe

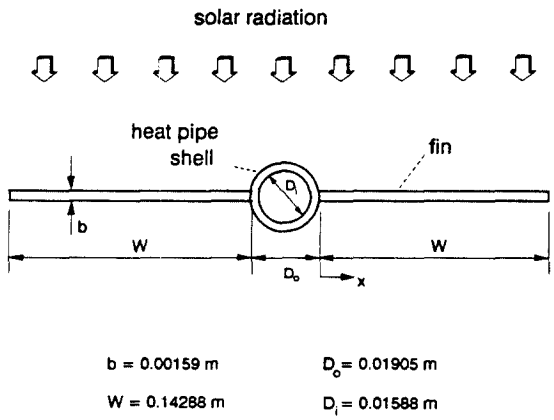

Fig. 1 Geometry of the heat pipe shell-fin cross-section

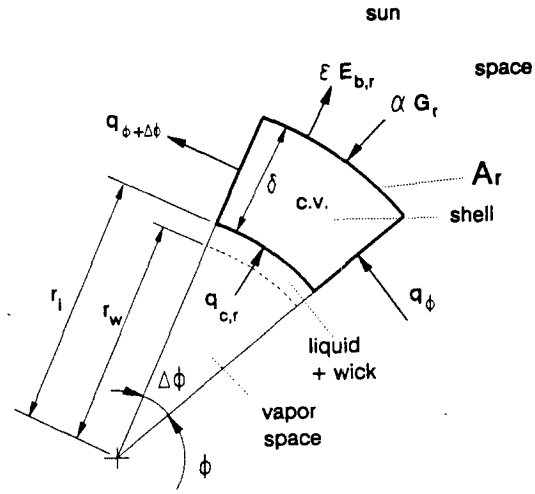

Fig. 2 Control volume for the analysis of heat pipe shell cross-section

shell is of interest. A significant simplification can be achieved in the solution procedure if the temperature variation is negligible in the curved heat pipe shell region. A two-dimensional analysis and numerical methods are employed to predict the thermal response of the structure. The procedure presented herein may be applicable to other problems subject to similar radiation boundary conditions.

The hot vapor flows through the core region of the heat pipe ($r<r_w$) surrounded by a liquid-saturated wick ($r_w<r<r_i$). The surfaces of the heat pipe shell ($r_i<r<r_o$) and the fins ($0<x<W$) are subject to uneven heat exchange. For space radiators, the upper surface is exposed to soloar radiation and space radiation while the lower surface is exposed only to space radiation. If a similar geometry is used for a heat pipe solar collector, the lower surface is usually insulated (Kanai et al., 1984, Duffie and Beckman, 1980). The heat pipe shell and the fins are considered to be made of the same material, typically an aluminum or its alloy the surface of which is treated to obtain a high emissivity (say 0.8) and a low absorptivity (say 0.3) for space radiators (Sadunas and Lehtinen, 1984). Typical values of the emissivity and the absorptivity of the solar collectors are about 0.2 and 0.9, respectively (Duffie and Beckman, 1980). The radiation properties of the surface are assumed uniform over the surface and constant so that they have neither spectral nor directional dependency.

Since the temperature distribution in the solid materials is of major concern in this study, the thermal effects of the vapor and liquid region inside the heat pipe are incorporated by assuming a bulk temperature of the vapor (T_v) and an overall heat transfer coefficient ($\bar{h}_c$) that accounts for the presence of the liquid-saturated wick. Thus, the radial heat flow from the vapor to the heat pipe shell (of temperature T_s) can be calculated by

$$q=\bar{h}_c A_c(T_v-T_s) \tag{1}$$

where A_c is the heat transfer area per unit axial length ($A_c=2\pi r_i$).

2. THEORETICAL ANALYSIS

The Biot number based on the eqivalent radiation heat transfer coefficient, Bi_{rad}, of the heat pipe shell in the radial direction and that of the fin in the direction normal to the surface are both very small ($Bi_{rad}\ll 10^{-4}$). Therefore the temperature differences in these directions are considered negligible (Özisik, 1980, Incropera and De Witt, 1990).

For a model geometry similar to the one used in this study, Sparrow and Cess(1966) examined radiant heat exchange between the curved pipe surface and the flat fin. Based on their analysis the model shown in Fig. 1 should have less than two percent of the overall rate of heat transfer from the fin affected by the existence of the curved pipe wall. Therefore the radiant interchange between the fin and the heat pipe shell surface is considered negligible.

Heat pipe shell :

For a differential element of the heat pipe shell shown in Fig. 2, an energy balance gives

$$q_\phi-q_{\phi+\Delta\phi}+(\alpha_r G_r-\epsilon E_{b,r})A_r+q_{c,r}=\rho c V\frac{\partial T}{\partial t} \tag{2}$$

where q_ϕ and $q_{\phi+\Delta\phi}$ are conduction heat transfer in the circumferential direction, and $q_{c,r}$ is convection heat transfer into the control volume (Siegel and Howell, 1981). In the above equation α_r and ϵ are the absorptivity and emissivity, respectively, $E_{b,r}$ is the blackbody emissive power, A_r is the area exposed to radiation, $2\pi r_o\Delta\phi$, and V is the volume. G_r is irradiation from the sun and space, i.e.,

$$G_r=G_{sun}\sin\phi+G_{space} \tag{3}$$

where G_{sun} is for a surface normal to the sun's ray and ϕ is 90° at the top of the curved surface and is 0° at the point where the fin is attached. Both G_{sun} and G_{space} values can be treated as knowns. For the radiator, G_{sun} is considered only on the upper surface ; for the solar collector, both G_r and $E_{b,r}$ are zero on the bottom surface since it is insulated.

Substitution of the geometrical parameters into Eq. (2) yields

$$k\delta\frac{1}{r_m^2}\frac{\partial^2 T}{\partial\phi^2}+(\alpha_r G_r-\epsilon\sigma T^4)\frac{r_o}{r_m}+\bar{h}_c\frac{r_o-\delta}{r_m}(T_v-T)$$
$$=\rho c\delta\frac{r_o}{r_m}\left(1-\frac{\delta}{2r_o}\right)\frac{\partial T}{\partial t} \tag{4}$$

where k is thermkal conductivity of the shell material, δ is the thickness of the shell, r_m is the center radius of the shell, $r_o-\delta/2$ and σ is the Stefan-Boltzmann constant.

$$\theta=\frac{T}{T_{ref}},\quad Fo=\frac{\alpha t}{W^2}\text{ and }\xi_r=\frac{r_o\Delta\phi}{W} \tag{5}$$

where α is the thermal diffusivity of shell material, W is the

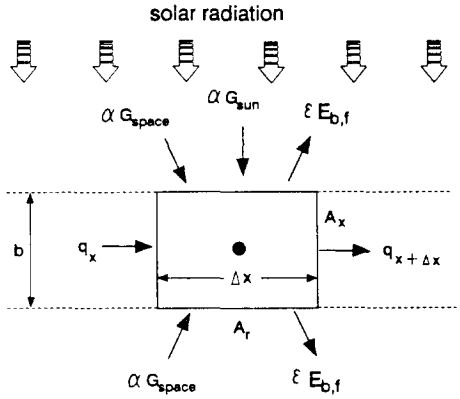

Fig. 3 Control volume for the analysis of the fin section

width of the fin, and T_{ref} is the reference temperature. Thus Eq. (4) can be reduced to the dimensionless form

$$\frac{\partial^2\theta}{\partial\xi_r^2}-\bar{S}_1\theta-\bar{S}_2\theta^4+(\bar{S}_1\theta_v+\bar{S}_o)=\bar{S}_3\frac{\partial\theta}{\partial Fo} \tag{6}$$

where

$$\bar{S}_o=(\alpha_r W^2 G_r/k\delta T_{ref})(1-\zeta/2)$$
$$\bar{S}_1=(Bi/(\delta/W)^2)(1-\zeta)(1-\zeta/2)$$
$$\bar{S}_2=(\epsilon\sigma T_{ref}^3 W^2/k\delta)(1-\zeta/2)$$
$$\bar{S}_3=(1-\zeta/2)^2 \tag{7}$$

In the above expressions, ζ is the thickness-to-radius ratio of the shell ($\zeta=\delta/r_o$) and Bi is the Biot number ($\bar{h}_e\delta/k$).

Fin section :

The energy equation for the fin section can be written as follows considering a control volume depicted in the Fig. 3. The conservation of energy principle for the control volume gives

$$q_x-q_{x+\Delta x}+(\alpha_r G_{r,f}-2\epsilon E_{b,f})A_r=\rho c V\frac{\partial T}{\partial t} \tag{8}$$

where q_x and $q_{x+\Delta x}$ are conduction heat transfer into and out of the control volume. $G_{r,f}$ is the total irradiation onto the fin surface which can be calculated by

$$G_{r,f}=G_{sun}+2G_{space} \tag{9}$$

for heat pipe radiators (see Fig. 3). For solar collectors, however, the second term on the right side of Eq. (9) is halved since the bottom surface of the fin is insulated. Eq. (8) can be arranged to yield a differential equation for the thermal behavior of the fin section

$$kb\frac{\partial^2 T}{\partial x^2}+\alpha_r G_{r,f}-2\epsilon\sigma T^4=\rho c b\frac{\partial T}{\partial t} \tag{10}$$

where b is the thickness of the fin.

With the dimensionless variable $\xi=x/W$ defined in addition to those of (5), Eq. (10) can be written in dimensionless form as

$$\frac{\partial^2\theta}{\partial\xi^2}-\bar{C}_1\theta^4+\bar{C}_o=\frac{\partial\theta}{\partial Fo} \tag{11}$$

where

$$\bar{C}_o=\alpha_r W^2 G_{r,f}/kbT_{ref} \text{ and } \bar{C}_1=2\epsilon\sigma T_{ref}^3 W^2/kb \tag{12}$$

3. NUMERICAL MODELING PROCEDURE

The finite difference method was used to solve the second-order nonlinear partial differental equations in this study. With a forward-time and center-space scheme (Carnahan et al., 1969, Jaluria and Torrance, 1986), Eq. (6) can be written in difference form as

$$\theta_j^{(n+1)}=\theta_j^{(n)}+\frac{\Delta Fo}{S_3}[\theta_{j-1}-(2+S_1)\theta_j+\theta_{j+1}-S_2\theta_j^4+(S_o+S_1\theta_v)]^{(n)} \tag{13}$$

where $S_k=\bar{S}_k\times(r_o\Delta\phi/L)^2$ for $k=0, 1, 2, 3$.

Eq. (13) may be simplified further as

$$\theta_j^{(n+1)}=M_o(\theta_{j-1}^{(n)}+\theta_{j+1}^{(n)})+M_1\theta_j^{(n)}-M_2\theta_j^{(n)4}+M_3 \tag{14}$$

where

$$M_o=\Delta Fo/S_3 \qquad M_1=1-M_o(2+S_1)$$
$$M_2=M_oS_2 \qquad M_3=M_o(S_o+S_1\theta_v) \tag{15}$$

Eq. (11), for the flat fin section, can also be reduced to a difference form as

$$\theta_j^{(n+1)}=N_o(\theta_{j-1}^{(n)}+\theta_{j+1}^{(n)})+N_1\theta_j^{(n)}-N_2\theta_j^{(n)4}+N_3 \tag{16}$$

where

$$N_o=\alpha\Delta t/(\Delta x)^2 \qquad N_1=1-2N_o$$
$$N_2=2\epsilon\sigma\alpha T_{ref}^3\Delta t/kb \qquad N_3=\alpha_r\alpha\ \Delta t\ G_{r,f}/kbT_{ref} \tag{17}$$

Nodal configuration for the numerical solution:

Since the relevant Biot numbers are very small, one node each in the radial direction for the heat pipe shell and in the direction normal to the surface for the fin is sufficient for the numerical analysis. The nodal configuration is shown in Fig. 4, which also illustrates the symmetry of the cross-section. An insulated boundary condition is applied at $j=1$ and $j=$NOP in the heat pipe shell and at $j=$NNA in the fin. At these nodes, a central difference yieds, $\theta_{j+1}=\theta_{j-1}$.

Steady-state solution :

For steady state, the right sides of Eqs. (6) and of (11) are zero, and the resultant difference equations for the heat pipe shell region can be written as

$$\theta_{j-1}-(2+S_1)\theta_j+\theta_{j+1}-S_2\theta_j^4+(S_o+S_1\theta_v)=0, \tag{18}$$

where S_k's are the same as those in (15). Similarly for the fin section

$$\theta_{j-1}-2\theta_j+\theta_{j+1}-C_1\theta_j^4+C_o=0 \tag{19}$$

where $C_k=\bar{C}_k(\Delta\xi)^2$ for $k=0$ and 1.

The shell node connected to the fin ($j=$NHP) must be treated separately since it has a convection boundary at one side and a conduction boundary at the other side. Radiation is neglected at this node although a fraction of its surface may be exposed to radiation if the node size is larger than that shown in Fig. 4. The finite difference equation at this node is

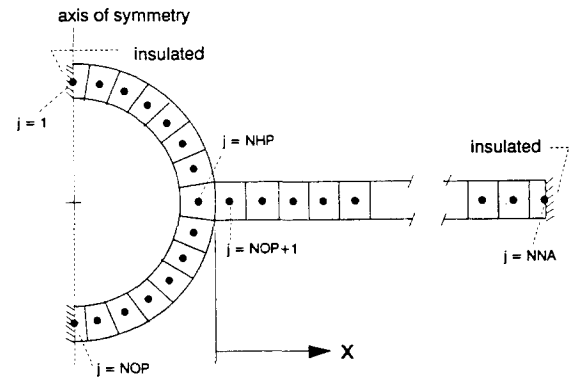

Fig. 4 Nodal configuration of the heat pipe shell-fin model

$$\theta_{NHP-1}-(2+S_1+S_{1m})\,\theta_{NHP}+\theta_{NHP+1}+S_{1m}\theta_{NHP+1}+S_1\theta_0=0 \tag{20}$$

where

$$S_{1m}=\frac{2b(r_0\Delta\phi)}{\delta(\delta+\Delta x)}\left(1-\frac{\delta}{2r_0}\right) \tag{21}$$

The solution strategy for the steady state problem involves an iteration procedure beacuse of the nonlinear term θ^4 in Eqs. (18) and (19). When applied to each node, Eqs. (18) through (20) result in a set of simultaneous equations of the form

$$[K]\{\theta\}^{(r+1)}=\{R\}^{(r)} \tag{22}$$

where $[K]$ is the coefficient matrix, $\{\theta\}$ is the column vector of unknown dimensionless temperatures and $\{R\}$ is the column vector consisting of constants and the nonlinear terms θ^4. Superscript (r) denotes the number of iterations. At each iteration step, the above matrix equation is solved by the LU decomposition method (Chapra and Canale, 1989). The convergence criterion for temperature is a dimensionless value of 10^{-5}.

The bulk temperature of the vapor inside the heat pipe is assumed to be 20°C and is kept constant. For solar collectors, however, the vapor temperature inside the heat pipe is assumed to be 50°C. Thus T_{ref} represents two different values, 293 K and 323 K, for the solutions of radiators and collectors, respectively. The overall heat transfer coefficient between the vapor and the heat pipe wall is assumed to be 3, 000 W/m²-K based upon data from technical reports (Sadunas and Lehtinen, 1984). The same value was used for the solar collector.

4. RESULTS AND DISCUSSION

Typical steady-state solutions are shown as dotted lines in Figs. 5 and 6 for a space radiator and a solar collector, respectively. The number of nodes in the heat pipe shell is 13 and that in the fin is 15. For the radiator, the values of the dimensionless parameters in Eqs. (7) and (12) are : $\bar{S}_0=0.08146$, $\bar{S}_1=147.262$, $\bar{S}_2=0.06796$, $\bar{S}_3=0.8403$, $\bar{C}_0=0.09216$, and $\bar{C}_1=0.1483$. For the collector, $\bar{S}_0=0.08146$, $\bar{S}_1=147.262$, $\bar{S}_2=0.06796$, $\bar{S}_3=0.8403$, $\bar{C}_0=0.1917$, $\bar{C}_1=0.04967$, while $\bar{S}_1$ and $\bar{S}_3$ values are the same as for the radiator. The results show that the difference between the maximum and minimum dimensionless temperatures in the heat pipe shell ($\xi<0$ in Fig. 5) is less than 1.3×10^{-3}(0.4 K) for the radiator, and the difference is less than 2.4×10^{-3}(0.8 K) for the solar collector. Therefore, circumferential temperature variations in the heat pipe shell may be neglected.

Since the numerical solutions for steady-state temperatures show that the heat pipe shell is nearly isothermal, the lumped heat capacity method (Myers, 1971, Incropera and De Witt, 1990) can be employed for the heat pipe shell region to reduce the computational time. The solution behavior in the curved shell region, however, depends on the dimensionless coefficients in Eq. (7). An independent effort is desired in this respect to identify the valid range of the lumped heat capacity method, in terms of those coefficients which account for the cases of similar geometries and boundary conditions. Thus, at the present time the validity of using the lumped method is limitd to the $\bar{S}_0$, $\bar{S}_1$, and $\bar{S}_2$ values as specified in the current study.

For the finite difference formulation, the lumped node can be treated as the first node in the fin having a mass and heat capacity equivalent to the whole heat pipe shell. The energy balance on the lumped node is

$$+kb\left(\frac{\partial T}{\partial x}\right)_{lumped}+\bar{h}_cA'_c(T_v-T)+\left[\alpha_r\left(\frac{G_{sun}}{\pi}+G_{space}\right)-\epsilon\sigma T^4\right]A'_r=(\rho cV)_{lumped}\frac{\partial T}{\partial t} \tag{23}$$

where $A'_r=\pi r_o-b$, $A'_c=\pi(r_o-\delta)$ and $(\rho cV)_{lumped}=\rho c\pi r_o\delta(1-(\delta/2r_o))$. The first term in Eq. (23) can be approximated by a forward difference as

$$+kb\left(\frac{\partial T}{\partial x}\right)_{lumped}\cong-kb\frac{T_1-T_2}{(\delta+\Delta x)/2} \tag{24}$$

where T_1 is the temperature of the lumped heat pipe shell and T_2 is the temperature of the first node in the fin. Then the dimensionless form of the Eq. (23) is obtained as follows by an explicit time marching scheme

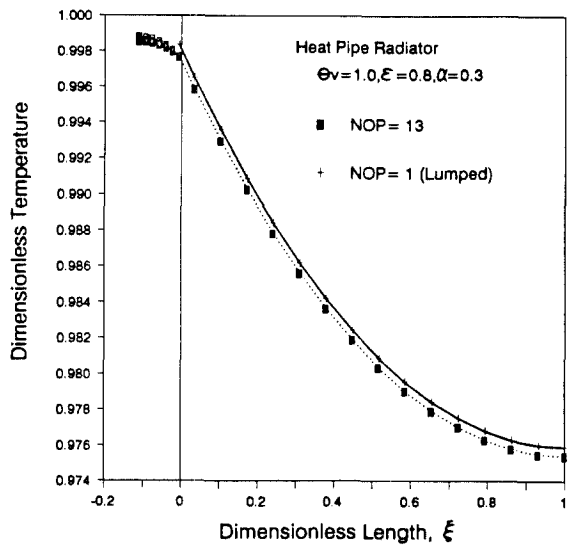

Fig. 5 Comparison of the steady-state solutions

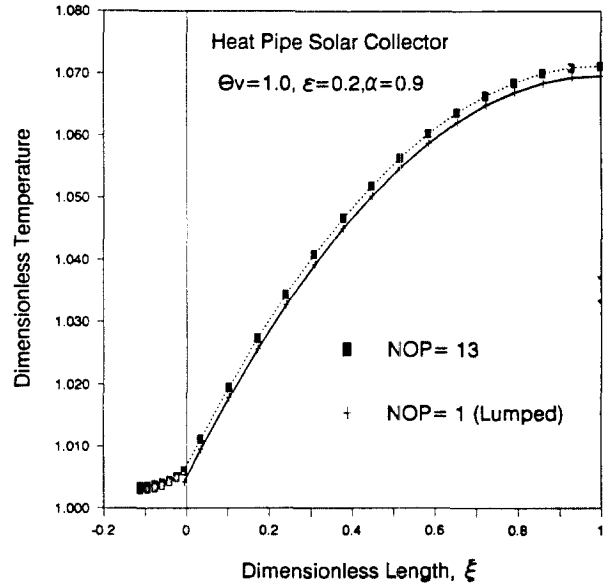

Fig. 6 Comparison of the steady-state solutions

$$\theta_i^{(n+1)} = B_o\theta_{i+1}^{(n)} + B_1\theta_i^{(n)} - B_2\theta_i^{(n)^4} + B_3 \text{ for } i=1 \quad (25)$$

where

$$B_o = H_1H_2$$

$$B_1 = 1 - H_2\left[H_1 + \bar{h}_c\left(\frac{r_i}{r_o}\right)\right] \qquad H_1 = \frac{2kb}{\pi r_o(\delta + \Delta x)}$$

$$B_2 = H_2\epsilon\sigma T_{ref}^3\left(1 - \frac{b}{\pi r_o}\right) \qquad H_2 = \frac{\Delta Fo W^2 r_o}{k\delta r_m}$$

$$B_3 = H_2\left[\bar{h}_c\left(\frac{r_i}{r_o}\right)\theta_v + \frac{dx}{T_{ref}}\left(\frac{G_{sun}}{\pi} + G_{space}\right)\left(1 - \frac{b}{\pi r_o}\right)\right] \quad (26)$$

In the Eq. (25), superscripts (n) and $(n+1)$ denote previous and present time steps, respectively.

To avoid poossible instabilities in the numerical solution, the gird Fourier number, $(\alpha\Delta t/(\Delta x)^2)$, has been maintained below 0.2 in this study. For steady-state solutions, Eq. (25) should be modified such that the left side of the equation is set to zero and the coefficient B_1 of the second term on the right side is reduced in value by subtracting 1. The resulting equation is then divided by H_2.

The numerical results from the lumped formulation are shown as solid lines in Figs. 5 and 6 to visualize the difference from those of the previous sormulation. The the largest temperature difference observed was about 0.12 K, which is negligible. Based on this observation, the following transient solutions are based on the lumped formulation.

Transient Solution Procedure :

For the transient analysis of the space radiators, initial

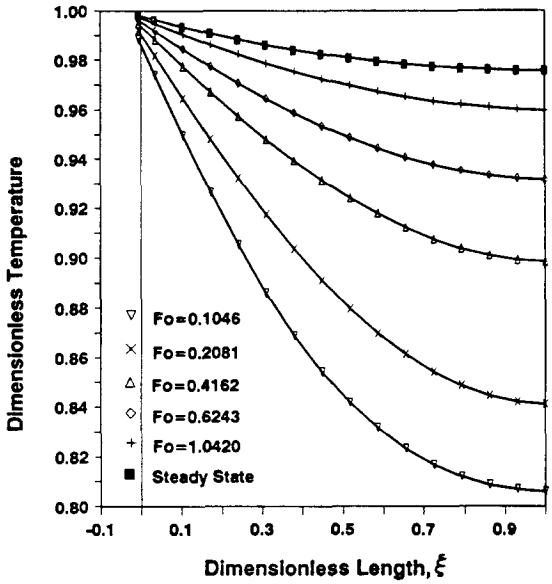

Fig. 7 Transient temperature characteristics of radiator(θv= 1.0, ε=0.8, α=0.3)

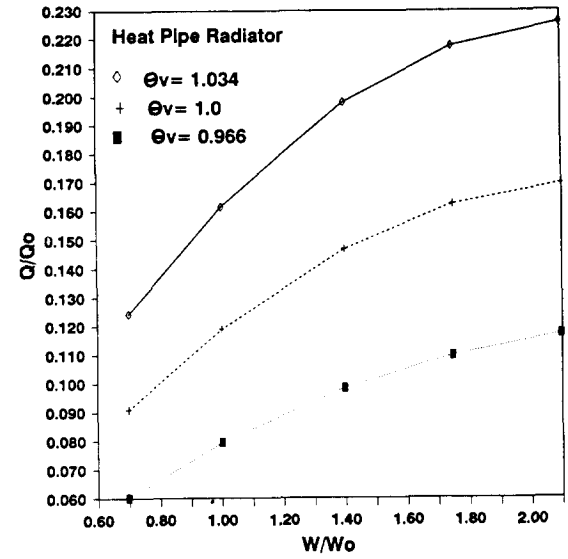

Fig. 9 Variation of heat transfer performance of heat pipe radiator

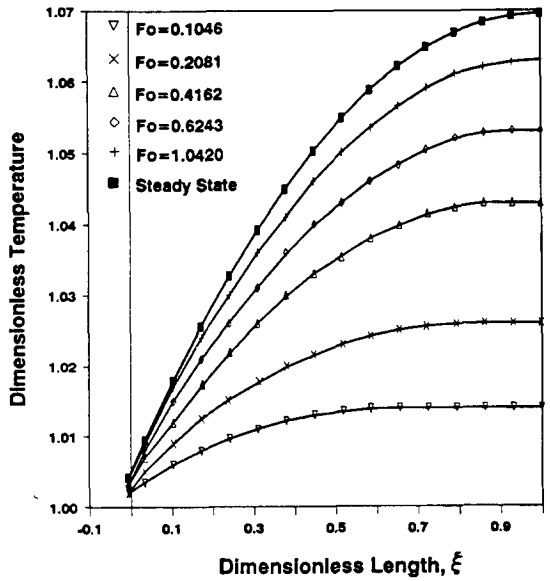

Fig. 8 Transient temperature characteristics of solar collector (θv=1.0 ε=0.2, α=0.9)

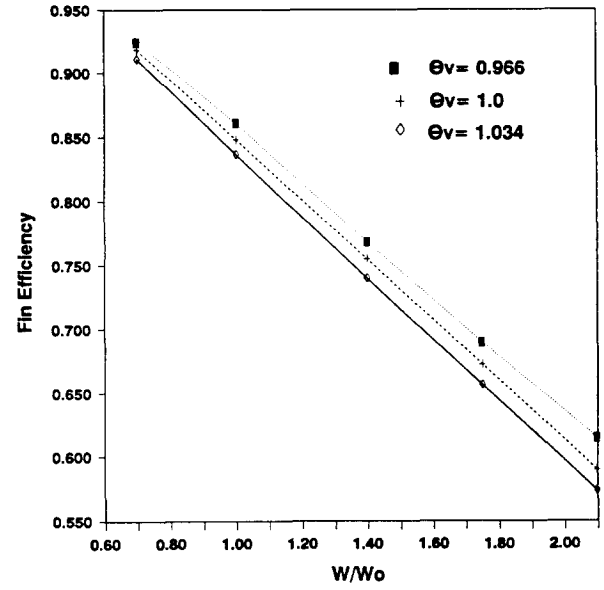

Fig. 10 Variation of radiator fin efficiency with fin width and heat pipe operating temperature

conditions are given such that the temperature throughout the heat pipe is the same as the space equivalent temperature (Sadunas and Lehtinen, 1984) of -40℃. Typical transient solutions are shown in the Figs. 7 and 8, for which the values of the dimensionless parameters in Eqs. (7) and (12) are the same as those for steady-state solutions. Fo in the Figures denote the dimensionless time and $Fo=1.0420$ corresponds to a real time of 254.5 seconds. The number of nodes placed in the fin section ($\xi>0$) is 15 and a lumped node ($\xi<0$) represents the heat pipe shell. As time progresses the transient temperature profile approaches the steady-state profile that was predicted by the lumped model and is shown as the top curves in Figs. 7 and 8.

The thermal performance of the heat pepe shell-fin structure were examined by varying the fin length, the heat pipe operating temperature, and typical surface properties associated with the radiation heat transfer. Fig. 9 shows that the heat transfer performance of the radiator increases with fin length, although the rate of increase attenuates. In this Figure, W_o is 0.14288 m as appeared in Fig. 1 and Q_o is defined as $\sigma(T_{ref}{}^4-T_\infty{}^4)$, where T_∞ is 233 K. The heat transfer rates are increased considerably with operating temperature, θ_v. For the dimensionless fin width, W/W_o, of 0.7, the heat transfer, Q/Q_o, increases by more than 50 percent for every 3.5 percent increase of θ_v from 0.966. And for $W/W_o=1.75$, the heat transfer is increased by 45 percent for every 3.5 percent increase of θ_v.

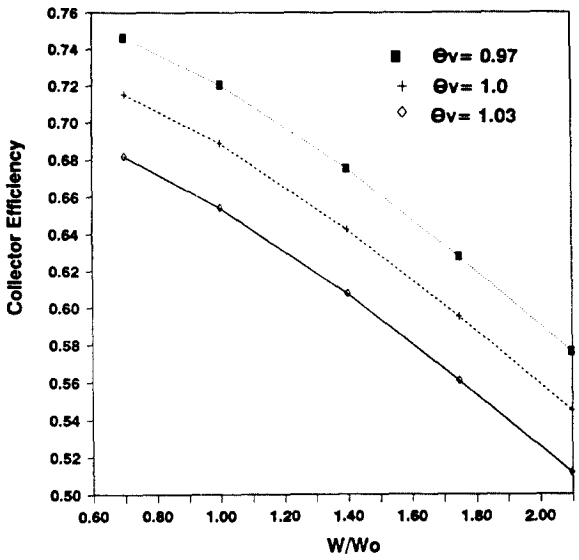

Fig. 11 Variation of collector efficiency with fin width and heat pipe operating temperature

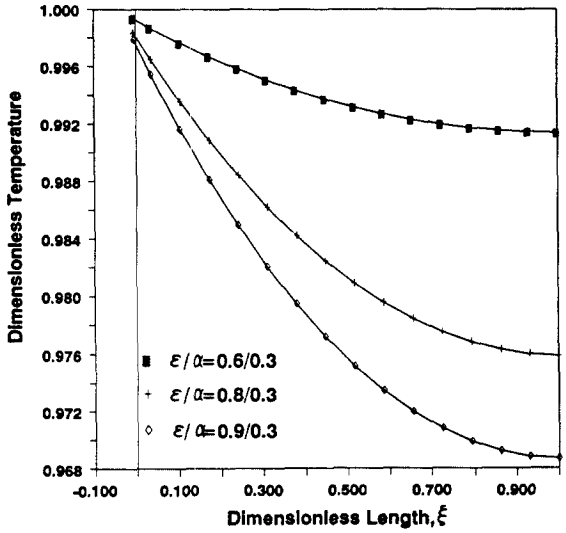

Fig. 12 Influence of surface properties on radiator temperature profiles

Figs. 10 and 11 exhibit fin efficiency and collector efficiency variations with fin width and operating temperatures. The fin efficiency is defined as the ratio of actual to the maximum possible heat transfer (Incropera and De Witt, 1990) while the collector efficiency is defined as the ratio of useful energy to the whole incident radiation on the surface (Duffie and Beckman, 1980). Efficiencies decrease with increasing fin width : The fin efficiency drops by 31 percent and collector efficiency drops by 17 percent as W/W_o is increased by 1.4, from 0.7. Efficiencies also decrease with increasing heat pipe operating temperature. Since the amount of maximum heat transfer through a fin is proportional to $(T_{base}-T_\infty)$ and T_{base} is nearly proportional to T_v, the efficiency would decrease as T_v increases unless the actual heat transfer through the fin surface increases at the same rate. On the other hand, since the amount of useful energy of a collector is proportional to (T_s-T_v), the collector efficiency would decrease as T_v increases unless the incident radiation on the surface increases at the same rate. The effect of operating temperature is less for the radiator (decrease by 1.0 percent for every 0.034 (10 K) increase in θ_v when $W/W_o=1.$) than for the collector (decrease by 4.2 percent for every 0.031 (10 K) increase in θ_v when $W/W_o=1.$).

The influence of the surface properties can be observed in Fig. 12 for the space radiator. As the emissivity-to-absorptivity ratio increases the temperature profile exhibits steep slope, which represents higher heat transfer. In dimensional values, heat rejection from the fin is increased from 10.7 W to 39.4 W (about 3.7 times). As the ϵ to α_r ratio increases from 0.2 to 0.3, (with $\alpha_r=0.3$), the temperature at the tip of the fin exhibits 0.022 (6.5 K) difference while the heat pipe shell temperature differs only by 2×10^{-3} (0.6 K).

5. CONCLUSIONS

(1) From the steady-state analysis the curved heat pipe shell was proved to be essentially isothermal. This result suggested that a lumped method can be used to simplify the mathematical model and to reduce associated computational expenses.

(2) The numerical results from the lumped capacity model showed that the predicted temperatures in the fin section were only about 0.12 K higher than the predicted values obtained with 13 nodes placed in the heat pipe shell region. However, this small variation had little impact on the thermal performance of the space radiators and solar collectors. Thus, it is concluded that the two-dimensional model can be simplified successfully to a one-dimensional model by thermally lumping the curved heat pipe shell.

(3) As time progresses, the transient temperature profile approaches the steady-state profile, thus exhibited qualita-

tively correct thermal behavior.

(4) For full analysis including three dimensions in space and time, i.e., when the temperature variation in the axial direction (which is normal to the paper in Fig. 1) is also of interest, the cross-sectional analysis as performed in this study can simplify associated effort a great deal.

(5) The fin efficiency decreases much rapidly with increasing fin length. As the heat pipe opeating temperature increases, both fin efficiency and collector efficiency decrease. In this case, the latter was more sensitive.

(6) The influence of the surface properties on the thermal performance of the shell-fin structure is very significant. Thus a proper selective coating technology can greatly enhance the thermal performance.

ACKNOWLEDGEMENT

This study was supported by the Korea Science and Engineering Foundation(KOSEF) under Grant Numer 903—0901—009—2, which is gratefully acknowledged.

REFERENCES

Carnahan, B., Luther, H.A. and Willkes, J.O., 1969, Applied Numerical Methods, John Wiley & Sons, New York.

Chapra, S.C. and Canale, R.P., 1989, Numerical Methods for Engineers, 2nd ed., John Wiley & Sons.

Colwell, G. T. and Hartley, J. G., 1988, "Development of an Emulation-Simulation Thermal Control Model for Space Station Application," Georgia Institute of Technology, Final Report submitted to NASA LaRC, under Grant NAG-1-551.

Duffie, J.A. and Beckman, W.A., 1980, Solar Engineering of Thermal Processes, pp. 197~281, John Wiley & Sons.

Incropera, F.P. and De Witt, D.P., 1990, Introduction to Heat Transfer, 2nd edition, pp. 226~236, John Wiley & Sons.

Jaluria, Y. and. Torrance, K.E., 1986, Computational Heat Transfer, Hemisphere Publishing Corp.

Kanai, T., Muramoto, H. and Saito, S., 1984, "Earth Embedded Cooling System and Solar Panels Using Heat Pipes," 5th International Heat Pipe Conference, Preprints III, pp. 62~68, Tsukuba, Japan.

Myers, G.E., 1971, Analytical Methods in Conduction Heat Transfer, McGraw-Hill.

Özisik, M. N., 1980, Heat Conduction, John Wiley & Sons, New York.

Sadunas, J. and Lehtinen, A., 1984, "High Efficiency Automated Thermal Control System Contract Critical Design Review (CDR) -DATA PACKAGE," Rockwell International Report No. SSD84-0161, Prepared for NASA JSC, December 7.

Siegel, R. and Howell J.R., 1981, Thermal Radiation Heat Transfer, 2nd edition, McGraw-Hill, New York.

Sparrow, E.M. and Cess, R. D., 1966, Radiation Heat Transfer, Brooks/Cole Publishing Company, Belmont, California.